Investigation of the Mechanism of Electrosynthesis of the Superconductor $Ba_{1-x}K_xBiO_3$

Gerald L. Roberts,[†,‡] Susan M. Kauzlarich,[*,†] Robert S. Glass,[*,‡] and John C. Estill[‡]

Department of Chemistry, University of California, Davis, California 95616, and Chemistry and Materials Science Department, University of California, Lawrence Livermore National Laboratory, Livermore, California 94550

Received June 10, 1993. Revised Manuscript Received August 24, 1993[⊗]

Cyclic voltammetry has been used to investigate the electrodeposition of the superconducting material, $Ba_{1-x}K_xBiO_3$. Reactions occurring at a Pt substrate electrode over a wide potential range have been assigned. Evidence has been found for time-dependent (cycle number) electrochemical behavior. High-quality superconducting crystals can be obtained only when the potential of the electrode is held in the region of predominantly kinetic control. The Bi^{III} to Bi^{V} oxidation appears as two peaks during the anodic scan. Reproducible cyclic voltammograms were obtained only after the KOH flux containing $Ba(OH)_2$ and Bi_2O_3 was equilibrated for 24 h under a water-saturated argon atmosphere. High-quality superconductive crystals are obtained only when the deposition potential is on the rising portion of the Bi^{III} to Bi^{IV} oxidation peak.

Introduction

The use of hydroxide fluxes for the synthesis of semiconducting and superconducting oxides has been investigated in several laboratories.[1–19] Recently, electrosynthesis has been used to grow large, single crystals of the superconducting compound, $Ba_{0.6}K_{0.4}BiO_3$ (BKBO).[20–26] As a preparative technique, molten salt electrodeposition has been studied extensively and reviewed.[27–31] Polycrystalline and single-crystal phases, which may not be prepared by direct solid-state methods, may be prepared via molten-salt electrolysis. Electrosynthesis has the potential advantages of greater control over the product stoichiometry, particle size, and morphology, compared to precipitation techniques.[31] Hydroxide fluxes dissolve metal oxides and tend to stabilize high oxidation states.[32,33] It has been shown that electrosynthesis of the $Ba_{1-x}K_xBiO_3$ superconductor from hydroxide fluxes can produce large single crystals that are required for the evaluation of fundamental properties.[23,34,35] BKBO crystals prepared by this technique have some of the highest superconducting transition temperatures (T_c's) observed to date.[16,22,23,36]

While electrodeposition of BKBO has been reported, there has been no attempt to investigate the processes occurring at the substrate electrode. In particular, cyclic voltammetry at "inert" electrodes that have been used as

[†] Department of Chemistry.
[‡] Chemistry and Materials Science Department.
* To whom correspondences should be addressed.
[⊗] Abstract published in *Advance ACS Abstracts*, October 1, 1993.

(1) Schneemeyer, L. F.; Thomas, J. K.; Siegrist, T.; Batlogg, B.; Rupp, L. W.; Opila, R. L.; Cava, R. J.; Murphy, D. W. *Nature* **1988**, *335*, 421.
(2) Ham, W. K.; Holland, G. F.; Stacy, A. M. *J. Am. Chem. Soc.* **1988**, *110*, 5214.
(3) Jones, N. L.; Parise, J. B.; Flippen, R. B.; Sleight, A. W. *J. Solid State Chem.* **1989**, *78*, 319.
(4) Lee, J.; Holland, G. F. *J. Solid State Chem.* **1991**, *93*, 267.
(5) Coppa, N.; Kebede, A.; Schwegler, J. W.; Perez, I.; Salomon, R. E.; Myer, G. H.; Crow, J. E. *J. Mater. Res.* **1990**, *5*, 2755.
(6) Wattiaux, A.; Fournès, L.; Demourgues, A.; Bernaben, N.; Grenier, J. C.; Pouchard, M. *Solid State Commun.* **1991**, *77*, 489.
(7) Cava, R. J.; Siegrist, T.; Peck, W. F., Jr.; Krajewski, J. J.; Batlogg, B.; Rosamilia, J. *Phys. Rev. B* **1991**, *44*, 9746.
(8) Nakamura, T.; Natsuhara, M.; Kawaji, H.; Itoh, M. *Jpn. J. Appl. Phys. Part 2-Lett.* **1991**, *30*, L1465.
(9) Carlson, V. A.; Stacy, A. M. *J. Solid State Chem.* **1992**, *96*, 332.
(10) Wignacourt, J. P.; Swinnea, J. S.; Steinfink, H.; Goodenough, J. B. *Appl. Phys. Lett.* **1990**, *53*, 1753.
(11) VerNooy, P. D.; Dixon, M. A.; Hollander, F. J.; Stacy, A. M. *Inorg. Chem.* **1990**, *29*, 2837.
(12) Pickardt, J.; Paulus, W.; Schmalz, M.; Schöllhorn, R. *J. Solid State Chem.* **1990**, *89*, 308.
(13) Bezzenberger, R.; Schöllhorn, R. *Eur. J. Solid State Inorg. Chem.* **1993**, *30*, 435.
(14) Kodialam, S.; Korthius, V. C.; Hoffmann, R. D.; Sleight, A. W. *Mater. Res. Bull.* **1992**, *27*, 1379.
(15) Lee, S. F.; Wei, J. Y. T.; Tang, H. Y.; Chien, T. R.; Wu, M. K.; Guan, W. Y. *Physica C* **1993**, *209*, 141.
(16) Han, P. D.; Chang, L.; Payne, D. A. *J. Cryst. Growth* **1993**, *128*, 798.
(17) Tang, H. Y.; Chen, W. L.; Chien, T. R.; Norton, M. L.; Wu, M. K. *Jpn. J. Appl. Phys. Part 2—Lett.* **1993**, *32*, L312.
(18) Mosley, W. D.; Dykes, J. W.; Klavins, P.; Shelton, R. N.; Sterne, P. A.; Howell, R. H. *Phys. Rev. B*, **1993**, *48*, 611.
(19) Marquez, L. N.; Keller, S. W.; Stacy, A. M.; Fendorf, M.; Gronsky, R. *Chem. Mater.* **1993**, *5*, 765.
(20) Norton, M. L.; Tang, H. Y.; Elgin, J. In *Chemistry of Electronic Ceramic Materials; NIST Special Publication 804*; Jackson, WY, August 17–22, 1990; p 413.
(21) Norton, M. L. *Mater. Res. Bull* **1989**, *24*, 1391.
(22) Norton, M. L.; Tang, H. Y. *Chem. Mater.* **1991**, *3*, 431.
(23) Mosley, W. D.; Liu, J. Z.; Matsushita, A.; Lee, Y. P.; Klavins, P.; Shelton, R. N. *J. Cryst. Growth* **1993**, *128*, 804.
(24) Rosamilia, J. M.; Glarum, S. H.; Cava, R. J.; Batlogg, B.; Miller, B. *Physica C* **1991**, *182*, 285.
(25) Nagata, Y.; Suzuki, N.; Uchida, T.; Mosley, W. D.; Klavins, P.; Shelton, R. N. *Physica C* **1992**, *195*, 195.
(26) Marcus, J.; Escribe-Filippini, C.; Agarwal, S. K.; Chaillout, C.; Durr, J.; Fournier, T.; Tholence, J. L. *Solid State Commun.* **1991**, *78*, 967.
(27) Crouch-Baker, S.; Huggins, R. A. *J. Mater. Res.* **1989**, *4*, 1495.
(28) Elwell, D. In *Crystal Growth and Materials*; Kaldis, E., Scheel, H. J., Eds.; North Holland: Amsterdam, 1976; p 606.
(29) Kunnmann, W. In *Preparation and Properties of Solid State Materials*; Lefever, R. A., Ed.; Dekker: New York, 1971; p 1.
(30) Wold, A.; Bellavance, D. In *Preparative Methods in Solid State Chemistry*; Hagenmuller, P., Ed.; Academic Press: New York, 1972; p 279.
(31) Feigelson, R. S. In *Solid State Chemistry, A Contemporary Overview*; Holt, S. L., Milstein, J. B., Robins, M., Eds.; American Chemical Society: Washington, DC, 1980; pp 243–276.
(32) Inman, D.; White, S. H. *J. Appl. Electrochem.* **1978**, *8*, 375.
(33) Trémillon, B. *Chemistry in Non-Aqueous Solvents*; D. Reidel: Dordrecht, Holland, 1974; pp 167–190.
(34) Cava, R. J.; Batlogg, B.; Krajewski, J. J.; Farrow, R. C.; Rupp, J. L. W.; White, A. E.; Short, K. T.; Peck, J. W. F.; Kometani, T. V. *Nature* **1988**, *332*, 814.
(35) Huang, Z. J.; Fang, H. H.; Xue, Y. Y.; Hor, P. H.; Chu, C. W.; Norton, M. L.; Tang, H. Y. *Physica C* **1991**, *180*, 331.
(36) Norton, M. L. In *Chemistry of Superconductor Materials*; Vanderah, T. A., Ed.; Noyes Publications: Park Ridge, NJ, 1992; p 347.

0897-4756/93/2805-1645$04.00/0

substrates to grow BKBO crystals from KOH–$Ba(OH)_2$–Bi_2O_3 melts has not been published. The possibility of time-variant electrochemical behavior, which could influence the properties of the materials deposited at constant potential, has not been explored. The relationship of the deposition potential to the mix of mass transport and kinetic factors controlling the rate of crystal growth has also not been explored. Lack of attention to these details has contributed to compositional inhomogeneities in the superconducting crystals produced by electrodeposition and continues to be a challenge in the $Ba_{1-x}K_xBiO_3$ system.[7,17,26] The most homogeneous crystals to date have been produced by top-seeded growth.[16]

In this work, we have used cyclic voltammetry to identify the electrochemical reactions occurring at platinum in the hydroxide melt in the anodic potential region. Variations in the voltammograms as a function of working electrode, flux composition, and time (scan number) have been explored. In addition, we have investigated the electrodeposition process as a function of potential.

Experimental Section

Apparatus. All electrodepositions were performed in a Teflon beaker (250-mL Nalgene Teflon-PFA type HP). The cell was equipped with a Plexiglas top through which the electrodes were fed. Uniform temperature was maintained by wrapping the beaker with electrical heating tape and heating the assembly from the bottom with a hot plate. Temperature was monitored at the beaker wall and bottom. The working electrode was a 0.3-mm-diameter Pt wire (0.048 cm^2 area exposed to solution). The counter electrode was a Pt wire (0.3-mm diameter, 0.48 cm^2 area exposed to solution) which was coiled around the working electrode. A Bi rod (5-mm diameter, Electronic Space Products International, 5 N purity) was used as the reference electrode.[20–22] Similar cells with a Pt counter and Bi reference electrode were also set up with Ag and graphite working electrodes. The Ag electrode was a 0.3-mm diameter wire (0.030 cm^2 area exposed to solution), and the graphite electrode was a rod (3.2-mm diameter, Graphite Specialty Products, Inc.). The graphite rod was enclosed in Teflon heat shrink tubing so that only the end of the rod was exposed to the solution. Cyclic voltammograms were obtained using an EG&G Princeton Applied Research Co. (PARC) Model 175 Universal Programmer, PARC Model 173 potentiostat/galvanostat, and Model 179 digital coulometer interfaced to a Zenith data systems computer. Constant electrolysis potentials were also set using this apparatus. All quoted potentials, unless otherwise stated, were measured with respect to the bismuth reference electrode. Data were collected, digitized, and analyzed using Labtech Notebook and Quattro.

Materials and Procedure. Prior to insertion into the cell, the working electrode was polished with 5.0-, 3.0-, 1.0-, and finally 0.5-μm alumina slurries. Semiconductor-grade KOH pellets (Aldrich, 99.99%), $Ba(OH)_2 \cdot 8H_2O$ (Aldrich, 98%), $Sr(OH)_2 \cdot 8H_2O$ (J. Matthey, Technical Grade), and Bi_2O_3 (Aesar, 99.9999%) were used to prepare the flux. The KOH pellets were placed in the cell and melted at 180 °C under water-saturated flowing argon. The KOH solution was stirred approximately 2 h with the three electrodes in place and with water-saturated argon flowing over the solution surface. $Ba(OH)_2 \cdot 8H_2O$ was then slowly added to the KOH solution followed by Bi_2O_3. The mole ratio of a typical melt was 34.95/0.54/1.00 (K/Ba/Bi, respectively).[21,22] After 24 h of stirring, to allow for maximum dissolution of the Bi_2O_3 and equilibration of the system, cyclic voltammograms of the quiescent solution were run to determine the electrocrystallization potential. Upon application of the chosen potential, the electrocrystallization process instantly initiated. Crystals were typically grown for more than 24 h, removed from the solution, and etched using a hot solution of disodium ethylenediamine tetraacetate (Na_2H_2EDTA).[24] Electrodepositions from both stirred and unstirred solutions were performed, and a comparison was made between the resulting crystal properties (lattice parameters and superconducting transition temperatures).

Characterization. Electrodeposited crystals were obtained at a constant potential for 3 h. The material was removed from the electrode and all of it ground into a powder for X-ray and magnetization measurements. In contrast to the results reported by others to date,[7,16–18,20–26] these measurements provide characterization of the entire electrodeposited material, not just selected single crystals. X-ray powder diffraction patterns of the materials were obtained using either an Enraf-Nonius Guinier camera (Cu $K\alpha_1$ radiation) or a Siemens D500 diffractometer (Cu $K\alpha$ radiation).

Magnetization studies were performed using a SQUID magnetometer (Quantum Design, Inc.). Samples were zero field cooled to 5 K and a 5-G field was applied. Magnetization measurements, as a function of temperature, were made up to 32 K.

Results and Discussion

Cell Setup. The argon atmosphere saturated with water vapor maintains an "inert" atmosphere and establishes a stable potential for the Bi reference electrode.[22] Electrocrystallization of superconducting phases of $Ba_{1-x}K_xBiO_3$ have also been reported when oxygen is present.[7,25] The cyclic voltammogram is similar to that observed for the cell with water-saturated argon flowing over it, but degradation of the Bi reference electrode is apparent. With water-saturated argon, no degradation was observed and Bi behaved as a stable reference electrode over the potential range studied (–0.2 to 1.0 V). Although we attempted to reproduce the experimental setup given by Nagata *et al.*, we were unable to obtain superconducting crystals with an applied potential of 1.00 V.[25] No further investigations of the effect of oxygen on the electrochemistry were performed.

Semiconductor grade KOH is important to use for the flux as it has been shown that small amounts of Na destroy the superconducting behavior in BKBO.[26,37] Small amounts of Na present in reagent-grade KOH produce a new phase that is reported to be perovskite-like with a = 8.54 Å.[26,37] We obtained crystals with similar lattice parameters using reagent grade KOH. The effect of the flux composition on the resulting crystal stoichiometry and superconductivity has been studied.[24] The optimal flux composition was determined to be 52.4/0.54/1.00 (K/Ba/Bi mole ratio) with the K/Ba ratio postulated as being the most important parameter for obtaining the superconducting BKBO phase, $Ba_{0.6}K_{0.4}BiO_3$.[24] We have found that the mole ratio composition of 34.95/0.54/1.00 (K/Ba/Bi, respectively)[21,22] provided the most homogeneous crystals with stoichiometries close to $Ba_{0.6}K_{0.4}BiO_3$ and this composition was used throughout the study. Bi^{III} is always in excess since it does not completely dissolve in the flux at 180 °C, even after 120 h, and probably in the form of the hydrate ($Bi(OH)_3$ or $Bi_2O_3 \cdot H_2O$).

The highest temperature that we employed for the electrodeposition of BKBO crystals was 180 °C. Although temperatures of 200–300 °C[20–26] have typically been used to grow superconducting crystals, we found 180 °C to be adequate.

We also investigated graphite as a working electrode in order to confirm peak assignments in the cyclic voltammogram. We found that the KOH solution turned black upon immersion of the graphite electrode, indicating dissolution of the graphite into solution, and a cyclic voltammogram could not be obtained using graphite as

(37) Chaillout, C.; Durr, J.; Escribe-Filippini, C.; Fournier, T.; Marcus, J.; Marezio, M. *J. Solid State Chem.* **1991**, *93*, 63.

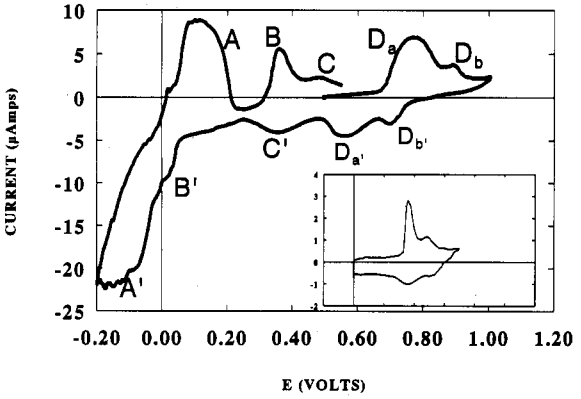

Figure 1. Cyclic voltammogram using a Pt electrode in a $Ba(OH)_2/Bi_2O_3/KOH$ solution. Scan rate = 50 mV/s. Inset shows the cyclic voltammogram using a Pt anode in a $Ba(OH)_2/KOH$ solution. The divisions are 0.2 V and the scan rate is 50 mV/s.

the anode. Although graphite crucibles have been successfully employed as the cathode for the electrosynthesis,[24] it was noted that the crucibles degrade and need to be replaced periodically. It has also been noted that graphite does not form a stable electrode material in hydroxide melts; it is easily oxidized to give carbonate ion.[38] Other groups have used a metal or graphite crucible as the cathode.[20-26,37] We found the three-electrode geometry described above to be sufficient to obtain superconducting crystals. All points on the surface of the anode are essentially equidistant from the surrounding, coiled cathode, providing nearly uniform current density which is important for the growth of symmetric, high-quality crystals.[39]

In this study, we have not performed a systematic evaluation of the effect of pH_2O on the electrochemistry. Clearly, it affects solubility and melt acidity, thus determining the composition of the electrodeposited phase.[2,26,40,41] At a minimum, the presence of a constant pH_2O and an otherwise inert atmosphere (Ar or N_2) results in a stable Bi reference electrode and inhibits oxidation of this material and other components of the melt.[20-22]

Cyclic Voltammetry. A typical cyclic voltammogram obtained in the $Ba(OH)_2$–Bi_2O_3–KOH electrolyte is shown in Figure 1. The initial potential of the voltammetric scan (0.50 V) was set at a value where no apparent electrochemical (anodic) processes occur; the potential range was swept first anodically up to 1.0 V, cathodically to −0.2 V and the cycle completed scanning anodically up to the initial potential. The following reactions[42-44] are proposed to occur:

peak A $$2Bi + 6OH^- = Bi_2O_3 + 3H_2O + 6e^- \quad (1)$$

peak B $$Pt + 2xOH^- = PtO_x + 2xe^- + xH_2O \quad (2)$$

peak C $$Pt + 2OH^- = Pt(OH)_2 + 2e^- \quad (3)$$

peak D $$\begin{cases} Bi_2O_3 + 2OH^- = Bi_2O_4 + H_2O + 2e^- & (4) \\ Bi_2O_4 + 2OH^- = Bi_2O_5 + H_2O + 2e^- & (5) \end{cases}$$

The peak labeling used in this work is outlined in the above reactions. The peaks designated by "primes" in Figure 1 indicate the reverse of the reactions. The identification of the peaks in Figure 1 was determined by performing cyclic voltammograms on a KOH solution, a $Ba(OH)_2$/KOH solution, a Bi_2O_3/KOH solution and a $Ba(OH)_2/Bi_2O_3$/KOH solution. In addition, a silver working electrode was investigated in order to facilitate identification of the peaks.

The anodic peak labeled A and the cathodic peak labeled A′ are straightforwardly assigned to the forward and reverse of reaction 1. Peaks labeled A/A′ were determined by scanning anodically from 0.00 to 0.20 V and cathodically from 0.20 to −0.20 V. The peaks are observed only when Bi_2O_3 is present in the solution.

Figure 1 (inset) shows the cyclic voltammogram obtained without any Bi present. The only peaks observed using a Pt electrode in a $Ba(OH)_2$/KOH melt consisted of the B/B′ and C/C′ couples. Peaks labeled C/C′ are present in KOH alone, whereas peaks labeled B/B′ are present only once $Ba(OH)_2$ has been added to the melt. The irreversible process represented by peaks B/B′ is probably associated with surface-localized processes, based upon the relative sharpness of the anodic peak, such as film formation/reduction. Peak B′ does not appear if the forward anodic scan is reversed prior to generation of peak B. An adsorption prepeak to peak B is sometimes apparent after the Bi_2O_3 is added to the solution. This may be due to a small amount of impurity or perhaps minor differences in the electrode surfaces from one experiment to the next, leading to a more gradual surface oxide formation in the oxide/hydroxide film formation region. Continued cycling and long equilibration times results in a decrease in the magnitude of peaks B and B′, again supporting the proposed assignment of peaks B/B′ to adsorption/film formation on the "bare" Pt substrate. In addition, a plot of peak current vs scan rate shows linear behavior consistent with a surface confined process (see supplementary material). It is likely that the peaks B/B′ are associated with the formation and dissolution of a protective platinum oxide/hydroxide film proposed in reaction 2.[45] The exact nature of the anodic film on platinum remains a controversial subject. However, several electrochemical steps are believed to be involved in the overall anodic oxidation process.[46] The role of Ba^{2+} in the adsorption/film formation is not fully understood, but since peaks B/B′ are observed only once $Ba(OH)_2$ has been added to the KOH melt, its presence appears to be important for the formation of an oxide film. It may play a role by shifting the equilibrium ($2OH^- \leftrightarrows H_2O + O^{2-}$) in the hydroxide melt.[40] To verify this hypothesis, we investigated the effect of $Sr(OH)_2$ on the cyclic voltammogram. However, $Sr(OH)_2$ is only very slightly soluble in KOH and no peaks were apparent in the cyclic voltammogram when it was added to the KOH melt.

Unlike peaks B/B′ which are only observed after $Ba(OH)_2$ is added to the solution, the peaks C/C′ are observed in all of the KOH solutions. The quasi-reversible C/C′

(38) Goret, J.; Trémillon, B. *Electrochim. Acta* **1967**, *12*, 1065.
(39) Sawyer, D. T.; Roberts, J. L., Jr. *Experimental Electrochemistry for Chemists*; Wiley-Interscience: New York, 1974; pp 78, 123.
(40) Plambeck, J. A. In *Encyclopedia of Electrochemistry of the Elements*; Bard, A. J., Ed.; Dekker: New York, 1976; Vol. X, p 283.
(41) Claes, P.; Glibert, J. In *Molten Salt Techniques*; Lovering, D. G., Gale, R. J., Ed.; Plenum Press: New York, 1983; Vol. 1, p 79–109.
(42) Milazzo, G.; Caroli, S. *Tables of Standard Electrode Potentials*; John Wiley & Sons: New York, 1978.
(43) Pourbaix, M. *Atlas of Electrochemical Equilibria in Aqueous Solutions*; Pergamon Press: New York, 1966; p 255–383.
(44) Latimer, W. M. *The Oxidation States of the Elements and their Potentials in Aqueous Solutions*, 2nd. ed.; Prentice-Hall: Englewood Cliffs, NJ, 1952; p 125.
(45) Kolthoff, I. M.; Tanaka, N. *Anal. Chem.* **1954**, *26*, 632.
(46) Be'langer, G.; Vijh, A. K. In *Oxides and Oxide films*; Vijh, A. K., Ed.; Marcel Dekker: New York, 1977; Vol. 5.

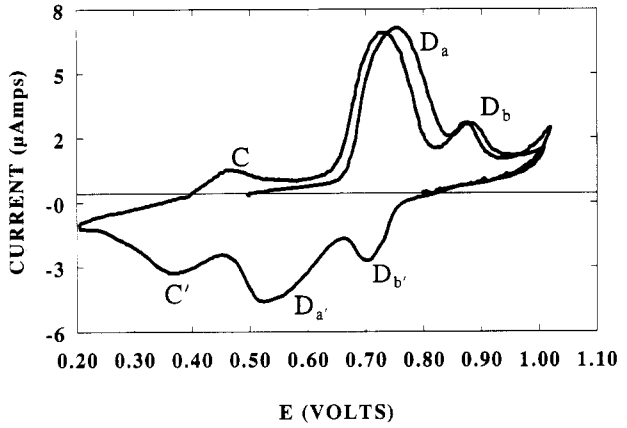

Figure 2. Cyclic voltammogram from 0.20 to 1.0 V using a Pt electrode in a $Ba(OH)_2/Bi_2O_3$/KOH solution. Scan rate = 50 mV/s.

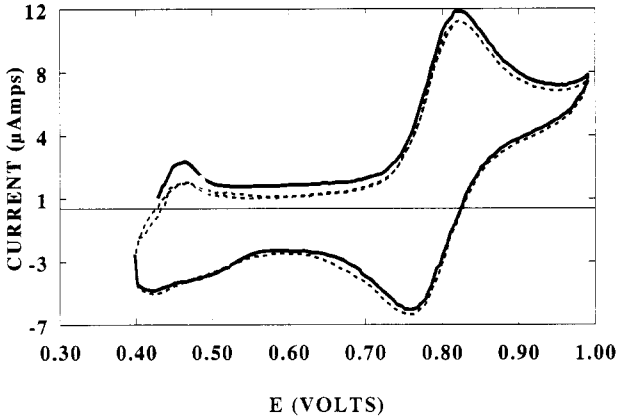

Figure 3. Cyclic voltammogram using a Pt electrode in a Bi_2O_3/KOH solution. Scan rate = 100 mV/s.

couple is present only after scanning cathodically to potentials less than 0.3 V and reversing the scan direction (Figure 2). The origin of the quasi-reversible peaks C/C′ is clearly due to a soluble redox couple, and the proposed redox eq 3 is given above. We propose that Pt-$(OH)_2$ is formed at the electrode surface, and it dissolves into the solution as a platinum hydroxide species such as $Pt(OH)_4^{2-}$.[47]

In hydroxide melts, Bi^{III} can exist as $BiOH^{2+}$, BiO^+, and Bi_2O_3, with the latter species dominating the equilibria.[48] Bi_2O_3 is only slightly soluble in the KOH–$Ba(OH)_2$ flux. Upon dissolution in KOH–$Ba(OH)_2$, Bi_2O_3 forms a hydrate, $Bi(OH)_3$ or $Bi_2O_3{\cdot}3H_2O$,[43] which appears as a white insoluble precipitate. In the absence of $Ba(OH)_2$ in the melt the Bi_2O_3 remains bright yellow. Although the assignments of the peaks to oxides (eq 4 and 5) are reasonable, it is probable that the reactions for the Bi(III)/Bi(IV) and the Bi(IV)/Bi(V) involve hydroxide species. Electrochemical oxidation of the Bi(III) species yields the Bi(IV) species, which may disproportionate to the III and V species. The quasi-reversible oxidation (a completely reversible system would have a peak separation of about 45 mV (for n = 2, 180 °C)) of this species is represented by peaks D_a/D_a' in Figures 1 and 2. Figure 2 shows two anodic scans of the bismuth region. To obtain a reproducible cyclic voltammogram the solution needed

(47) Kozawa, A. *J. Electroanal. Chem.* **1964**, *8*, 20.
(48) Bard, A. J. *Encyclopedia of Electrochemistry of the Elements*; 1986; Vol. IX, Part B.

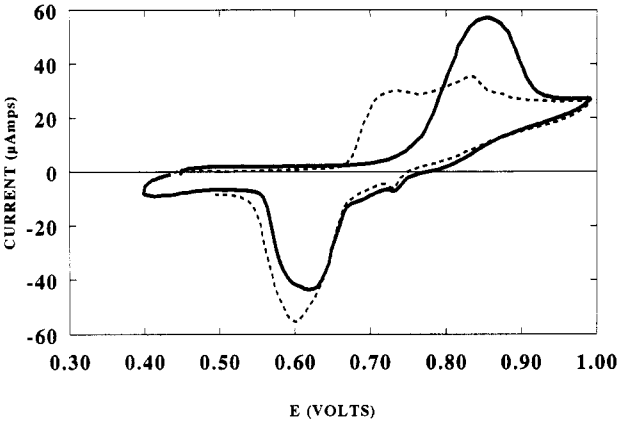

Figure 4. Cyclic voltammogram using a Pt electrode in a Ba-$(OH)_2/Bi_2O_3$/KOH solution shortly after $Ba(OH)_2$ is added. Solid line represents first scan; dashed line represents second scan; scan rate = 100 mV/s.

to be equilibrated with H_2O saturated Ar. With time, a brownish blue-black precipitate is formed, indicating that chemistry takes place even without an applied potential. The shift of both anodic peaks to less positive values during the second scan may imply the presence of a more favorable surface for oxidation, likely an oxide layer or BKBO deposited material.[39] It is possible that the species generated in the first peak is further oxidized to give the second peak.

To identify the species giving rise to the cyclic voltammogram in Figures 1 and 2, we performed cyclic voltammetry in the flux without $Ba(OH)_2$. The cyclic voltammogram of the flux with the Bi_2O_3–KOH combination is shown in Figure 3 and exhibits only one reversible redox couple in the bismuth region that is independent of scan rate, as well as length of time the melt is stirred at constant temperature. The single anodic peak is indicative of only one bismuth species present in the solution. We believe the anodic peak is due to the straightforward oxidation of Bi^{III} to Bi^V in which there is significant overlap of the processes represented by eq 4 and 5. Our assignment is supported by the fact that we were able to electrodeposit single crystals of $KBiO_3$, a Bi(V) compound, on the rise of the anodic peak (0.78 V). The electrodeposition of $KBiO_3$ has been previously reported.[14] The large crystals appear black on the surface but are orange powders when ground. The lattice parameter for the cubic crystals, as determined by powder X-ray diffraction, is a = 10.038(2) Å, slightly larger than that reported by Kodialam *et al.*[14]

Two peaks begin to appear in the voltammetric scans as soon as $Ba(OH)_2$ is added (Figure 4). The process also immediately becomes quasi-reversible. A single broad anodic peak is present during the first scan (scan rate = 100 mV/s) that shifts to lower potential during the second scan, splitting into two peaks of approximately equal magnitudes. As mentioned previously, the cyclic voltammograms are time dependent. Over 24 h the cyclic voltammogram will eventually look like that shown in Figure 2, where the peaks are no longer of equal magnitude. The exact role of Ba^{2+} is not fully understood, but it is apparent that its presence changes the shape of the cyclic voltammograms, as well as the chemical processes occurring in the bismuth region.

Previous studies have used Ag as a working electrode in the successful electrocrystallization of BKBO[22] and $KBiO_3$[14] although the mechanisms involved were not

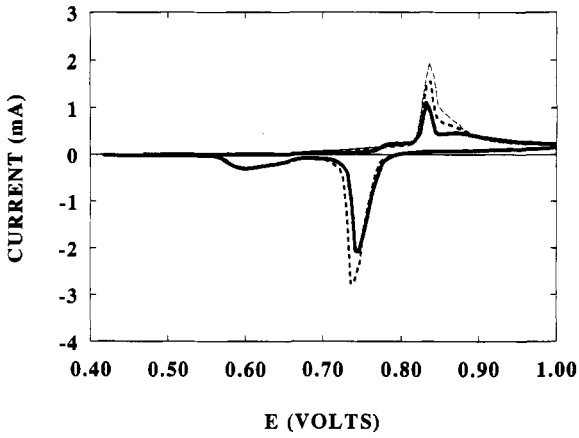

Figure 5. Cyclic voltammogram of the $Ba(OH)_2/Bi_2O_3$/KOH solution with a Ag wire as the anode, Pt wire as the cathode and Bi reference electrode. Scan rate = 100 mV/s. First, second, and third scans are indicated by solid, bold dashed, and dashed lines, respectively.

explored. We have also examined the electrochemistry of BKBO crystal growth using Ag as a working electrode and the cyclic voltammogram of this system is shown in Figure 5. Since silver corrodes in molten hydroxide fluxes, the solution was first allowed to equilibrate for 24 h, and then the Ag electrode was partially submerged and the cyclic voltammogram immediately taken. Cyclic voltammograms were also taken of the KOH, and $Ba(OH)_2$–KOH solutions without any Bi. The peaks observed in the 0.4–1.0-V region occur only once Bi_2O_3 is added to the solution and are attributed to Bi^{III} to Bi^{V} oxidation, and subsequent reduction. Two oxidation peaks are present in the first anodic scan through the bismuth region, as well as all subsequent scans. Unlike the Pt electrode, a shift to lower potentials is not observed during continuous cycling for the Ag anode. In addition the peak shapes remained constant, thereby implying that the surface of the Ag electrode is not modified by the flux, unlike the Pt electrode. The broad peak, in the case of the Ag substrate, clearly represents the diffusional oxidation process. The sharp peak, in the case of the Ag substrate, indicates that there is a large fraction of current coming from an adsorbed species. The peak currents are several orders of magnitude greater when Ag is employed as the working electrode (μA on Pt vs mA on Ag for identical cell configurations and electrode areas). The peak currents also increase with scan number through the bismuth region, in contrast to behavior observed using a Pt electrode, implying a large surface area which may be a result of the buildup of an insoluble product on the substrate. The shapes of cyclic voltammograms are also modified in ways that are characteristic of the electrode mechanism. Such modifications may be the result of chemical reactions preceding, following, or coupled to the charge transfer and adsorption of the reactive species.

Constant-Potential Electrodeposition. The electrocrystallization of BKBO is initiated by the proposed oxidation of Bi^{III} to Bi^{IV}. As a result of favorable Madelung energies, the spectator ions, Ba^{2+} and K^+, are readily incorporated into a growing three-dimensional crystal mass. The relative adsorption of Ba^{2+} and K^+ on the corners of the cubic close-packed structure, and therefore the rate of growth, varies with the concentration of the ions in solution. Maintenance of constant melt activities and other parameters, such as stirring rate (mass transport), temperature, etc., during crystal growth should produce high-quality homogeneous cubic crystals. In principle, electrocrystallization offers considerable control over the rate of crystal growth, particularly because the electrodeposition potential directly controls the potential. For instance, at relatively low potential in the Bi^{III} to Bi^{IV} oxidation region (for instance, at 0.68 V—see Figure 1), the crystal growth will be dominated by kinetic limitations. At higher positive potentials (for instance >0.80 V), the crystal growth is dominated by mass transport considerations. At intermediate potentials, crystal growth will be influenced by both of these factors.

Table I. Lattice Parameter and T_c Onset as a Function of Electrodeposition Potential

electrodeposition potential, V	Lattice parameter (powder diffraction), Å	T_c onset,[a] K
0.60	4.392(3)	
0.65	4.293(1)	20
0.68	4.287(3)	28
0.70	4.286(3)	16
0.75	4.284(5)	20
0.775	4.282(1)	23
0.80	4.279(1)	22
0.85	4.277(1)	

[a] T_c onset values are from individual plots of χ_g vs temperature.

In addition to the above considerations, small amounts of impurities added with reagents may significantly affect superconductive properties. For instance, as mentioned previously, incorporation of Na^+ into the growing crystal is known to reduce the superconductivity onset temperature in the $Ba_{1-x}K_xBiO_3$ system.[26,37] Impurities may also be contributed by oxidation of the substrate electrode on which the crystals grow. Soluble complexes of Pt or Ag are possible when these materials are used as the anode; however, neither of these elements were detected by X-ray fluorescence in the BKBO crystals grown in this study.

Following attainment of a steady-state voltammogram upon repeated cycling, crystal growth was initiated at constant potentials in the (primarily) kinetically controlled, mixed, and mass-transport-dominated regions for the oxidation of Bi^{III} to Bi^{IV}. In relation to Figure 2, this corresponds to the potentials on the rising portion of the first oxidation peak (i.e., at 0.68 V), at the peak potential and somewhat beyond (e.g., 0.72, 0.74 V) and at potentials between the two peaks (i.e., 0.85 V). Table I shows the lattice parameters obtained, using powder X-ray diffraction, for material deposited on the anode as a function of the applied potential. The gradual decrease in size of the cell, with increasing electrodeposition potential, indicates that a greater portion of Bi(III) is being oxidized to Bi(V) and deposited at the substrate. The composition, deduced from the lattice parameters, corresponds to increasing x in $Ba_{1-x}K_xBiO_3$. As previously mentioned, the stable Bi(V) compound, $KBiO_3$, is capable of being electrodeposited at 0.78 V in the absence of $Ba(OH)_2$. In addition, a new phase begins to grow in at 0.75 V and is present in significant amounts in the 0.85-V crystal deposits, as evidenced by powder X-ray diffraction. This new phase can be indexed as an orthorhombic lattice with a = 13.944(2), b = 13.247(2), and c = 8.077(1) Å. In contrast to the crystals grown at 0.68 V, those grown at higher potentials are easily dislodged from the electrode surface. Table I also shows T_c's for the electrodeposited material. The T_c's reach a maximum for the material deposited at 0.68 V. Although the T_c's are high for the material deposited at 0.75–0.80 V, the fraction of superconducting material

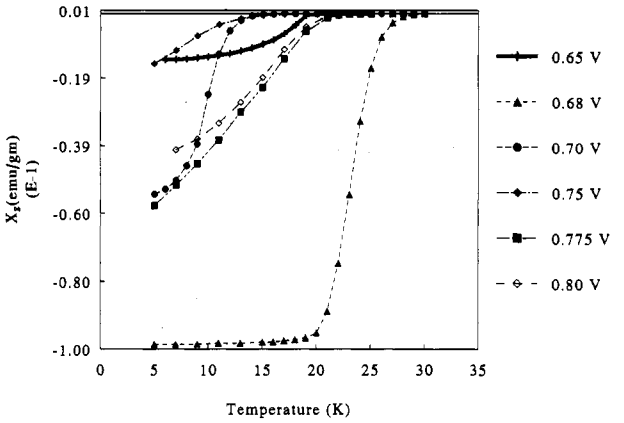

Figure 6. T_c is a function of electrodeposition potential for crystals grown at constant potential between 0.65 and 0.80 V for 3 h.

is small. This is shown in Figure 6.

Electrocrystallization at potentials in the primarily kinetically controlled region results in crystals which are superconducting, while those grown at higher potentials (>0.80 V) where mass transport begins to dominate are nonsuperconducting. We found no significant differences in the quality of crystals grown in either a stirred or quiescent solution at 0.68 V. This is expected since crystal growth in this potential region is dominated by kinetic factors. In general, crystals that were grown for short periods of time (24 h or less) resulted in lower T_c onsets and inhomogeneous barium concentration (determined from microprobe studies). These findings are similar to those reported by others.[22,24,37] In the present study, the minimum electrodeposition time necessary to obtain superconducting crystals was found to be 0.25 h (T_c onset = 20 K), and the maximum time was 120 h (T_c onset = 30.5 K). Crystals electrodeposited on the platinum substrate varied in color from black to blue and golden bronze on the surface. The outer surface coloring was also found to be dependent upon processes involved in the postelectrodeposition. The golden bronze surfaces could be removed to obtain sharper T_c's. The crystals could be manually separated and identified microscopically. Concentration gradients throughout the bulk electrodeposited material were confirmed by electron microprobe analysis. Similar results as a function of deposition time have been observed in other laboratories.[22,23,25] It has been shown that subsequent annealing of the crystals in an oxygen atmosphere at 400 °C for 2 h increases and sharpens the T_c substantially.[23] Superconducting crystals (T_c onset = 18 K) were grown at 0.77 V using Ag as the working electrode.

In several experiments the current was monitored as a function of electrodeposition time, while maintaining constant potential. A rapid nonlinear increase in current is observed during the initial growth stages. Maximum current is achieved and persists for a number of hours (typically 48–92 h), during which time the more homogeneous phases of $Ba_{1-x}K_xBiO_3$ are believed to be electrodeposited. This type of nucleation phenomenon is typical in random 3-D inhomogeneous crystal growth.[31] After depletion of the Ba^{2+} ions in the flux, the current density decreases in a nonlinear fashion and potassium rich phases are produced.

Summary

Cyclic voltammetry has been used to investigate the mechanism for electrochemical synthesis of superconducting $Ba_{1-x}K_xBiO_3$ from KOH–$Ba(OH)_2$–Bi_2O_3 melts. Electrochemical processes occurring on two different substrate materials, Ag and Pt, were explored over a wide potential range. While Pt is not inert in this media, no effect on the superconducting properties of the electrodeposited crystals was noted.

The assignment of the peaks B/B′ and C/C′ (Figure 1) to electrochemistry involving the platinum substrate is supported by several observations. The peaks are observed with only KOH and $Ba(OH)_2$ present in solution. Neither K^+ nor Ba^{2+} is expected to have any significant oxidation or reduction chemistry in hydroxide melts.[40] No peaks are observed in the same potential regions when Ag is used as the working electrode. In addition, the peaks B/B′ are greatly diminished on subsequent scans, indicating that the electrode is becoming passivated with respect to the electrochemical reactions responsible for these peaks. Typically, peak B′ is smaller than peak B, indicating incomplete removal of the surface oxide by cathodic scanning. This effect has previously been noted for Pt in alkaline media.[47] Continued cyclic scanning results in decreased magnitudes and eventually the absence of peaks B/B′.

It was found that the Bi^{III} to Bi^{V} oxidation, which initiates crystal growth, appears as two peaks in the anodic and cathodic scans for scans beginning in the region preceding the anodic peaks as well as in the region between the two peaks. The two anodic peaks, which are present only after $Ba(OH)_2$ is added, could be attributed to (1) the presence of two bismuth species that do not exhibit reversible behavior or (2) the formation of a surface layer of oxide or BKBO on the electrode which can be further oxidized to give the second peak. Furthermore, crystals with good superconducting properties (T_c's about 30 K) can be obtained under potentiostatic conditions only if the electrodeposition potential is chosen so that the oxidation of Bi^{III} to Bi^{IV} is primarily kinetically controlled (potentials on the rising portion of the Bi^{III} oxidation peak). Electrodepositions at higher potentials produce cubic and orthorhombic phases of $Ba_{1-x}K_xBiO_3$. The lattice parameter of the cubic material decreases with increasing electrodeposition potential, favoring a more complete oxidation to the Bi^{V} state or greater doping of K beyond the superconducting stoichiometries.

Acknowledgment. We thank R. N. Shelton for the use of his magnetometer and X-ray diffractometer, and H. B. Radousky, P. Klavins, W. R. Fawcett, and G. B. Balazs for useful discussions. Financial support from the National Science Foundation (DMR-8913831, 9201041) is gratefully acknowledged. This research was performed under the auspices of the U.S. Department of Energy of the Lawrence Livermore National Laboratory under Contract W7405-ENG-48.

Supplementary Material Available: Figures with varying sweep rates are provided for the KOH–$Ba(OH)_2$–Bi_2O_3 flux (4 pages). Ordering information is given on any current masthead page.